



A possible approach to improving rotating disc contactor design accounting for drop breakage and mass transfer with contamination

J.S. Ghalehchian, M.J. Slater*

Department of Chemical Engineering, University of Bradford, Bradford, W.Yorks BD7 1DP, UK

Accepted 30 June 1999

Abstract

A model of a liquid–liquid rotating disc contactor is postulated which takes into account drop breakage but not coalescence, individual drop motion and contact time in a stage, mass transfer coefficients which are affected by contamination, and axial mixing in the continuous phase only. The model is intended to guide industrial design work under conditions of interfacial contamination which are expected in industrial practice: academic work has concerned itself primarily with very clean systems resulting in mass transfer correlations which are not appropriate for industrial design work. The work addresses the question whether mass transfer data obtained experimentally for single drops can be used with confidence in column design. It is shown that average drop sizes and hold-up can be simulated well without using adjustable parameters for each experiment for hold-up not exceeding 20%. The mass transfer performance can be modelled using a contamination factor which varies with drop diameter and residence time; however, the effect of contamination is apparently reduced in the RDC perhaps by virtue of reduced contamination gradient on the drop surface brought about by non-uniform drop motion. The work indicates that mass transfer data for single drops in vertical motion may not be valid for column design (although giving conservative results) unless drops can be shown to be very clean in both cases. © 1999 Elsevier Science S.A. All rights reserved.

Keywords: Liquid-liquid extraction; Rotating disc contactor; Drop mass transfer

1. Introduction

Much progress has been made in recent years in modelling the various aspects of performance of liquid–liquid extraction columns [1]. The processes of single drop breakage and mass transfer to single drops in particular are better understood. Characteristic velocities for isolated drops in columns and axial mixing coefficients in both phases have been correlated by ourselves and other workers for a wide range of column diameters, particularly for the rotating disc contactor. One important phenomenon which has not been adequately studied is that of coalescence between drops and the consequences for both hydrodynamic and mass transfer performance. This study sought to avoid conditions in which drop coalescence could be expected to occur so that conclusions on drop size, hold-up and mass transfer behaviour could be more reliably drawn.

A test of adequacy of modelling concepts and empirical equations and an important engineering requirement is to simulate the performance of existing columns (usually only

data from small diameter laboratory equipment are available) without using adjustable parameters specific to each system or individual experiment. Otherwise pilot plant information will always be necessary for design of large columns. Two major problems are to be confronted – the effects of interdrop coalescence and the effects of interfacial contamination on mass transfer coefficients. In this work, we have chosen to side-step the question of coalescence between drops by considering only normal operating conditions of dispersed phase hold-up of less than 20% and mass transfer direction into solvent drops. As has been shown by a number of investigators [2,3,4] the rate of coalescence of drops is much lower when the mass transfer direction is from the aqueous continuous phase into the droplet phase, which is the case for experiments in this study. We have employed a model of mass transfer coefficients which takes into account interfacial contamination and which recognizes the time-dependency of the drop mass transfer coefficient, both of which are important in describing extraction column behaviour. Using the life-time of every drop (between breakages or severe disturbance by rotors, both tending to render drop concentrations uniform) renders calculations very lengthy; in this work residence time in each compartment is used as a

*Corresponding author.

E-mail address: m.j.slater@bradford.ac.uk (M.J. Slater)

simplifying assumption. This work explores the use of this model applied to counter-current extraction in a 23 compartment RDC of 152 mm diameter.

It is necessary to construct a simulation model to explore the validity of the multiplicity of equations used in computations and to help judge where deficiencies lie. There is a strong interaction between individual process aspects in extraction equipment. It is very difficult, if not impossible, to determine the absolute effect of every parameter involved. This work illustrates the application of a detailed description of mass transfer coefficients coupled with calculation of changing drop size distributions (due to breakage only) and individual drop velocities. Progress in understanding coalescence in swarms of drops undergoing mass transfer can only be made by simulation studies which incorporate well-founded descriptions of the other processes involved – drop breakage and motion, mass transfer and axial mixing [5]. Even then, there remains the problem of coupling of mass transfer and coalescence. The final resolution of this problem is therefore not yet within reach but there are current industrial demands for better guidance on design, particularly for the mass transfer calculations, which have somehow to be met.

2. Column performance models

For the simulation and design of liquid–liquid extraction columns the discrete character of the drops (different residence times, velocities and different modes of mass transfer), has to be recognized as shown by Rod [6], Misek and Rod [7], and Misek and Marek [8] for example and reviewed by Pratt and Stevens [9]. Relevant studies of RDCs have been carried out by Korchinsky and Azimzadeh-Khatayloo [10], Chartres and Korchinsky [11], Cruz-Pinto and Korchinsky [12] Korchinsky and co-workers [13–15], Zhang et al. [16] and by us. The work on packed and pulsed columns carried out by Hamilton and Pratt [17], Garg and Pratt [18], Yu and Wang [19] is also of considerable value. However, none of this work by others attempts to take account of the effect of contamination on mass transfer coefficients.

Gourdon et al. [20] have developed a very detailed model which includes the effects of inter-drop coalescence as well as drop breakage. The current limitations are the assumption of an overall mass transfer coefficient which does not properly account for individual drop behaviour, and the use of a coalescence rate equation (derived by data fitting) which may be physically unrealistic. However, the calculation framework using a full drop population balance has been firmly established. Other researchers continue to work on the problem [21,22].

Talib [23] has used a stagewise contact model with forward mixing of dispersed phase, taking into account the effect of drop breakage to give a varying distribution of drop sizes along the column. The work has been extended

to a steady-state approach by Ghalehchian [24] on the basis described below.

3. Model equations for drop hydrodynamics

We have to start by considering the inlet drop size to the first compartment of a column. In this case the inlet drop size was unknown since no dispersed phase distributor was used, as is common industrial practice. An estimate of maximum likely drop size in the column was made using the equations provided by Chang-Kakoti et al. [25] and this was used as a uniform inlet drop size, the largest expected value. We have used the equations

$$d_{\max} = 2.4d_{32}^{0.8} \quad (\text{diameters in mm}) \quad (1)$$

(together with measured d_{32} for steady size distribution) and

$$d_{\max} = 2.0 \left(\frac{\gamma}{g\Delta\rho} \right)^{0.5} \quad (2)$$

using the higher value of d_{\max} in calculations of developing size distributions. The choice of inlet drop size is not vitally important in estimating drop sizes in most of the column compartments.

Cauwenberg et al. [26] have presented the equations for single drop breakage probability, daughter drop size distributions and critical conditions for breakage for non-mass transfer and mass transfer conditions that are used in calculations. For breakage probability, p , the form of the equations is

$$\frac{p}{(1-p)} = b(We_d - We_{d_{CR}}) \quad (3)$$

(b varies with column diameter and rotor Reynolds number, see [26]). For critical conditions the rotor speed N_{CR} at which drops of diameter d start to break is given by

$$2\pi N_{CR} = \frac{0.802\gamma^{0.70}}{\rho_c^{0.30}\mu_c^{0.40}d^{0.59}D_r^{0.71}} \quad (4)$$

For the mean number of daughter drops

$$x_m = 2.0 + 0.9 \left(\frac{d_M}{d_{CR}} - 1 \right) \quad (5)$$

For daughter drop size distribution

$$fr(x_m, y) = (x_m - 1)(1 - y)^{x_m - 2} \quad (6)$$

The mean characteristic velocities were determined using the equation given by Godfrey and Slater [27] for each of the 10 drop size classes considered in the size distribution.

$$\frac{V_k}{V_t} = 1.0 - 1.443(N_r^3 D_r^5)^{0.30} - 0.494 \left(\frac{d}{D_s - D_r} \right)^{0.77} \quad (7)$$

The slip velocity equation used for all drop sizes was taken from the same source;

$$V_{\text{slip}} = V_k(1-x)^n \quad (8)$$

$$n = 0.19Re_k^{0.5} \quad (9)$$

All these equations were combined as discussed by Talib [23] to calculate the drop size distribution varying along the column. Ten drop size classes of equal length were used since 10 was sufficient to give good representation of hydrodynamics within the experimental error; class length ratios of 0.8 to 1.2 showed no influence on calculated results.

4. Model equations for mass transfer calculation

The stagewise model described by Korchinsky and Azimzadeh-Khatayloo [10] was employed in this work. Forward mixing of drops was assumed, for which any drop fraction interval with an average size d_i and rising velocity $V_{d_i,n}$ passes through any stage, n , in a plug flow manner. Individual drop velocities for a given drop size vary slightly through the stages, as the interfacial tension varies due to mass transfer.

The following main assumptions were adopted:

1. Constant net phase volumetric flow rates;
2. Constant temperature and other physical properties except the interfacial tension;
3. Mass transfer of one solute and interfacial contamination expected;
4. Drops are spherical and there is no coalescence of drops;
5. Drop contact time for mass transfer coefficient estimation is residence time in a compartment.

Axial mixing in the continuous phase was modelled using the stage back-flow ratio, e . The backmixing for dispersed phase was reasonably assumed to be negligible as assumed by a number of authors [6,11,28,29].

Fig. 1 shows a typical stage, n , in which an element of height, dh , is considered. For one drop size, d_i , with real velocity $V_{d_i,n}$ we use

$$E = \frac{C_{d_i,n} + C_{d_i,n-1}}{C_{d_i,n}^* - C_{d_i,n-1}} = 1 - \exp\left(\frac{-6K_{od_i,n}h_c}{V_{d_i,n}d_i}\right), \quad (10)$$

$$n = 1, \dots, N_{st}$$

together with solute balances. The equations were solved to obtain the concentration profiles along the column [24].

5. Mass transfer coefficients

Mass transfer coefficients for a swarm of drops of a range of sizes are normally estimated using several empirical

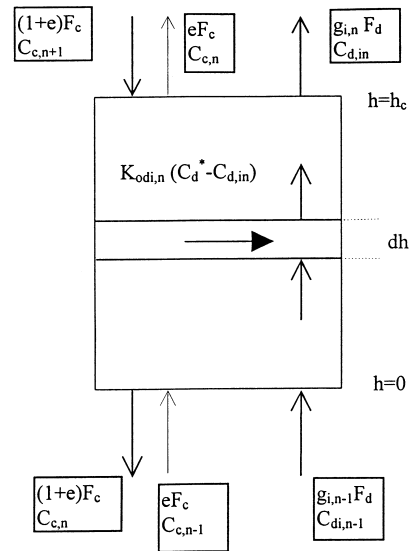


Fig. 1. Mass transfer model in stage n .

equations with unlikely sharp transitions from one to another, and with no clear linkage between continuous phase and dispersed phase coefficients [30]. This situation is quite unsatisfactory for design problems since the proper conditions of application are uncertain and there is no recognition of the effect of interfacially active contaminants likely to be of importance in industrial systems. Only the trial and error fitting of these equations to single drop or drop swarm mass transfer data can show which are relevant. Several pairs of such equations are usually needed to cover a range of drop sizes.

A combined mass transfer coefficient model recently proposed by Slater [31] was developed to resolve this difficulty in a practical manner. Two equations only are used, needing specification of one unknown contamination factor which clearly links behaviour in the two phases. The model allows for contamination of the drop interface and the residence time of the drop in a stage which are considered to be key elements of successful representation of mass transfer in industrial extraction columns.

For the continuous phase the film mass transfer coefficient is here given by a modified potential flow solution. The adsorption of surface active material at the interface on a moving drop results in a contaminant concentration gradient which reduces circulation inside drops. For this condition [32] has derived the equation

$$Sh = \frac{2}{\sqrt{\pi}} \alpha^{1/2} Re^{1/2} Sc^{1/2} \quad (11)$$

where

$$\alpha = \frac{V_{\text{int}}}{V_t} = 1 - \frac{2 + 3(\mu_d/\mu_c) + m}{1 + (\rho_d\mu_d/\rho_c\mu_c)^{1/2}} \frac{1.45}{Re^{1/2}} \quad (12)$$

valid for α only slightly less than 1.0. V_{int} is the average interfacial velocity and V_t the terminal velocity; m is the

dimensionless contamination factor. Eq. (12) may only be suitable for low levels of contamination factor m and high Re numbers. The equation may give negative values of α at low Re numbers (order 10) which is the case for a range of drop sizes in operating columns. Slater [31] has therefore proposed an alteration to Eq. (12) to avoid this problem and allow use of Reynolds numbers of about $1 < Re < 1000$ and high values of m ;

$$Sh = \frac{2}{\sqrt{\pi}} \left[1 + \frac{2 + 3(\mu_d/\mu_c) + m}{1 + (\rho_d\mu_d/\rho_c\mu_c)^{1/2} Re^{1/2}} \frac{1.45}{Re^{1/2} Sc^{1/2}} \right]^{-0.5} \quad (13)$$

The Eq. (13) is based on using the approximation $\alpha = 1 - x = (1 + x)^{-1}$ valid for small x values. It is here proposed to apply the Eq. (13) also to conditions of any value of x giving $0 < \alpha < 1$. The parameter m needs to be determined from experimental data. A value of $m = 0$ is appropriate for clean drops and a value of several hundred is used to simulate a near rigid drop. Eq. (13) has been fitted to the experimental data (with a wide range of Re) for single drop mass transfer collected by Steiner [33] with an average value of about 20 for m (with considerable scatter of data) [31] so the proposal to use Eq. (13) is considered reasonably well-founded and the approximation for α at high x values is of practical value for current purposes.

The contamination factor m has a physical meaning since the general definition is

$$m = -\frac{\beta(\partial\gamma/\partial\Gamma)}{\mu_c^2} \quad (14)$$

where

$$\beta = \frac{2\Gamma_0\mu_c r_0}{3[2D_s + \varepsilon D_B r_0^2 / \{D_B + \varepsilon\delta(\partial\Gamma/\partial C_{eq})\}]} \quad (15)$$

It is unrealistic however to think that the values of the contaminant diffusivities D_s and D_B and the factors Γ_0 , ε and δ could be measured so they are lumped into the parameter β , and in this work into the contamination factor m , to allow application to industrial systems. It can be understood that m is likely to be a function of drop radius r_0 and interfacial contamination gradient changing with time so an empirical equation (see Eq. (20) below) is used in fitting concentration profile data.

There is a lower limit for Sh for rigid drops ($\alpha \rightarrow 0$). Based on the experimental data provided from different sources, Steiner [33] has modified an equation given by Kinard et al. [34] for rigid drops to give the form which is used in this work;

$$Sh_r = 2.43 + 0.775Re^{1/2}Sc^{1/3} + 0.0103Re Sc^{1/3} \quad (16)$$

Eq. (16) is used instead of Eq. (13) when $Sh < Sh_r$ for any particular drop size.

The continuous phase film mass transfer coefficient needs to be combined with the time-dependent coefficient for the

drop since resistance to mass transfer is significant in both phases in the butanol system used in this work; resistance lies principally in the dispersed phase for the cumene system also used. The required overall mass transfer coefficient K_{odi} can be calculated using addition of resistances (Whitman two-film theory) or the direct mathematical solution of diffusional mass transfer in spherical drops in which solute is transferring to or from the continuous phase offering finite mass transfer resistance;

$$K_{odi} = \frac{d_i}{6t_i} \ln \left\{ \sum_{n=1}^{\infty} \frac{6L^2}{\beta_n^2[\beta_n^2 + L(L-1)]} \exp\left(-\frac{4D_d\beta_n^2 t_{r,i}}{d_i^2}\right) \right\} \quad (17a)$$

$$\beta_n \cot\beta_n + L - 1 = 0 \quad (17b)$$

$$L = \frac{k_{ci}d_i}{2\Phi D_c} \quad (17c)$$

which shows a dependency of K_{odi} on contact time as well as drop size [33]. The time used in calculations of K_{odi} is that for a drop to pass through a stage (based on drop velocity). This is an assumption which can be challenged but true drop life-times cannot be easily calculated because not all drops break at each rotor. This assumption is the same as assuming that concentrations in drops in each class are made uniform after each stage as if drops were newly formed at each rotor; it is considered that the disturbance or breakage suffered by drops when passing each rotor renders internal concentrations of drops uniform. The number of terms used in Eq. (17a) was eight and the series converged rapidly even with short contact times for large drops. However, the first three terms are the most important in calculation.

We use an overall diffusivity D_{oe} which is the sum of molecular and eddy diffusivity. The eddy diffusivity due to circulation, D_e , is defined according to the ideas of Handlos and Baron [35] for single vigorously circulating drops, as:

$$D_e = \frac{dV_t}{2048(1 + (\mu_d/\mu_c))} \quad (18)$$

The factor 2048 in Eq. (18) is a consequence of improper boundary conditions assumed by Handlos and Baron as explained by Hubis and Hartland [36], and it changes if other approximations are made. However, fortuitously perhaps, the Handlos and Baron equation generally works very well. The overall effective diffusivity taking contamination into account is then

$$D_{ce} = D_d + \alpha D_e \quad (19)$$

and D_{oe} is used in Eq. (17a) instead of D_d . When $Sh < Sh_r$ the value of α does not exactly equal zero but D_{oe} is put equal to D_d to be consistent. The use of Equations (13) and (17a) provides a straightforward method of accounting rationally for the effects of contamination on both film coefficients over the whole range of behaviour of rigid to fully-circulating drops.

Young and Korchinsky [37] proposed an alternative effective diffusivity model which was dependent on rotating disc agitation power input, drop size and the interfacial tension. It requires a parameter which must be determined from experimental data. Temos et al. [38] suggest a similar procedure but neither method deals explicitly with the problem of contamination.

6. The contamination factor determination

The combined film mass transfer model described above has been used by Slater and Hughes [39] for assessing single drop mass transfer using the butanol–succinic acid–water system, and by Alessi et al. [40] for cumene–phenol–water, and cumene–acetone–water, in both cases by fitting the model to experimental results with a suitable contamination factor, *m*. The work of Slater and Hughes [39] indicated that a near-linear dependency of *m* on contact time with a non-linear dependency on drop size best represented the values of contamination factor. It is reasonable to expect that *m* should increase as drops adsorb more contaminants from the aqueous stream as time passes. Small drops are less sensitive to contamination since circulation in drops is inhibited at small diameter. In this work a generalized correlation in a form showing a dependence on time and drop size needed as noted above was therefore applied:

$$m = m_o + a_1 t d^{a_2} \tag{20}$$

where *t* in s; *d* in mm, in which parameters *m_o*, *a₁* and *a₂* were determined by fitting experimental concentration profiles. It seems totally impractical to predict or correlate values of *m* using physical properties alone. It is unfortunate but necessary that the effects of contamination have currently to be correlated empirically for the chemical system used.

7. Continuous phase backflow parameter

The relationship between axial mixing coefficient, *E_c*, and backflow parameter, *e*, derived by Miyauchi and Vermeulen [41] is used:

$$\frac{E_c}{V_c H} = \frac{e + 0.5}{N_{st}} \tag{21}$$

Table 1
The backflow ratio for runs of the butanol–succinic acid–water system

Run No.	<i>F_d</i> = <i>F_c</i> (cm ³ /s)	<i>N_r</i> (s ⁻¹)	Hold-up, <i>x</i>	<i>e</i>	
				Kumar and Hartland	Misek
L8	59.12	0.42	0.281	0.602	0.108
L9	50.78	0.42	0.159	0.579	0.126
L10	33.73	0.42	0.082	0.542	0.190
L11	59.12	0.00	0.181	1.865	0.000
L12	42.25	0.83	0.177	0.534	0.299
L13	25.40	0.83	0.075	0.622	0.498

Two correlations are used:

1. The correlation of Misek [42] which was developed for a range of rotating disc contactor and asymmetric disc column sizes from 50 to 2180 mm in diameter given by Eq. (21) with:

$$e = \left(\frac{0.00679}{h_c}\right)^{1/3} \left(\frac{N_r D_r}{V_c}\right) \left(\frac{D_r}{D_{col}}\right)^{2/3} \left(\frac{D_s}{D_{col}}\right)^2 \tag{22}$$

2. The correlation of Kumar and Hartland [43] which was developed based on 1055 data points for 32 liquid systems obtained by 19 investigators in both rotating disc and asymmetric rotating disc contactors of diameter 41 to 2180 mm. It is given by:

$$\begin{aligned} \frac{E_c}{V_c h_c} = & 0.42 + 0.29 \frac{V_d}{V_c} + \left[0.0126 \frac{N_r D_r}{V_c} + \frac{13.38}{3.18 + (N_r D_r / V_c)} \right] \\ & \times \left(\frac{V_c D_r \rho_c}{\mu_c}\right)^{-0.08} \left(\frac{D_{col}}{D_r}\right)^{0.16} \left(\frac{D_{col}}{h_c}\right)^{0.10} \left(\frac{D_s}{D_{col}}\right)^2 \end{aligned} \tag{23}$$

where $\bar{V}_c = V_c / (1-x)$ is the continuous phase velocity relative to the column. The correlation is shown by Kumar and Hartland to predict the behaviour of continuous phase at low agitation particularly well and it is shown by the authors that mass transfer does not affect the axial mixing coefficient.

The continuous phase backflow parameters of butanol–succinic acid–water and cumene–isobutyric acid–water runs are given in Tables 1 and 2.

8. Experimental data

Experimental results are available from experiments done for Separation Processes Service (SPS), AEA Technology, Harwell by the University of Bradford. The 152 mm diameter pilot column used was made of pyrex glass and was fitted with 23 equal compartments with constructional details as given in Table 3 [44].

Cumene (iso-propylbenzene)–isobutyric acid–water was one of the systems examined which has a relatively high interfacial tension and very low mutual solubility. The second system used was butanol–succinic acid–water with a low interfacial tension and partial mutual miscibility (inlet flows were therefore mutually saturated). The mass transfer

Table 2
The backflow ratio for runs of the cumene–isobutyric acid–water system

Run No.	$F_d = F_d/3$ (cm ³ /s)	N_r (s ⁻¹)	Hold-up, x	e	
				Kumar and Hartland	Misek
H9	13.90	4.16	0.031	0.96	1.52
H10	20.80	4.16	0.059	0.65	1.02
H11	27.75	4.16	0.090	0.50	0.76
H12	16.64	5.00	0.045	0.95	1.53
H13	20.80	5.00	0.061	0.76	1.22
H14	6.65	5.41	0.025	2.66	4.14
H15	9.97	5.41	0.036	1.74	2.76
H16	13.33	5.41	0.073	1.28	2.06

direction was from continuous to dispersed solvent phase. All the experiments were conducted at about 20°C.

The physical properties of both systems are given in Table 4. For the mass transfer runs the appropriate average physical properties at the solute concentrations at top and bottom of the column were used.

The equilibrium distribution for succinic acid between water and butanol (at 20°C) is given by

$$C_d = 1.086C_c - 0.849 \times 10^{-3}C_c^2 - 0.162 \times 10^{-4}C_c^3 \quad (24)$$

where C_d and C_c are concentrations of succinic acid in butanol and aqueous phases respectively in kg/m³, $C_c < 50$ kg/m³. For isobutyric acid distribution the equilibrium data (20°C) are fitted with the equation:

$$C_d = 0.135C_c^{0.85} \quad (25)$$

C_d and C_c in kg/m³ isobutyric acid; $C_c < 50$ kg/m³.

The experimental results are listed in Tables 5 and 6. The experimental and computed plug flow values of the overall number of transfer units N_{odp} were used as one indication of closeness of simulation. Hold-up and drop size data are given in [3].

A problem was that the inlet and outlet measured concentrations did not provide a 100% solute mass balance, while the calculated values were in perfect mass balance. In order to achieve the 100% solute mass balance around the column, the continuous and dispersed phase outlet concentrations were adjusted, since they are most subject to error, as shown in Table 5. The concentration profiles were used to judge how to make these minor adjustments. All concentration profile data were used in the model-fitting discussed below.

Table 3
Dimensions of the RDC

Column diameter (mm)	152
Rotor diameter (mm)	102
Rotor thickness (mm)	3.18
Stator inner diameter (mm)	111
Minimum free area (%)	53
Compartment height (mm)	76
Column working height (mm)	1750

9. Modelling of hydrodynamics of mass transfer runs

Bahmanyar et al. [45], Bahmanyar and Slater [46], Cauwenberg [47] and Cauwenberg et al. [48] have studied the influence of mass transfer on the drop breakage in RDCs. It is reported that drop breakage probability for systems with mass transfer can be modelled in the same way as for no mass transfer conditions, if the change of interfacial tension is taken into account. A linear variation of interfacial tension through the column, between those values appropriate to solute concentrations at the inlet and outlet continuous phase was used. For cumene–isobutyric acid–water system the interfacial tensions were between about 15 to 20 and for butanol–succinic acid–water between about 0.8 to 1.4 mN/m. Ideally the interfacial tension should be made a measured or predicted function of concentration.

Presented in Table 6 are the calculated column average hold-up and overall Sauter mean drop size, with experimental results for comparison. For three runs of the butanol–succinic acid–water system with agitation speed of 0.42 s⁻¹ the experimental maximum drop size is smaller than critical drop size near the bottom of the column ($\gamma \cong 1.4$ mN/m) and is only slightly more than critical drop size at the top of the column ($\gamma \cong 0.8$ mN/m). For these three runs and the run L11 in which the agitation speed is zero, no drop breakage by rotor agitation is predicted so the Mugele and Evans [49] drop size distribution was assumed (brought about by natural break-up of drops in the inlet region).

The generated hold-up and Sauter mean diameters in every stage for a number of runs are illustrated in Figs. 2 and

Table 4
Physical properties of both systems for mass transfer runs at 20°C

Physical property	Cumene–isobutyric acid–water system	Butanol–succinic acid–water system
ρ_c (kg/m ³)	1000.0	991.0
ρ_d (kg/m ³)	867.0	865.0
μ_c (mPa s)	1.06	1.55
μ_d (mPa s)	0.81	3.65
D_c (m ² /s)	0.79×10^{-9}	0.52×10^{-9}
D_c (m ² /s) ^a	1.11×10^{-9}	0.22×10^{-9}
γ (mN/m)	15.0–20.0	0.80–1.40

^aMass transfer conditions.

Table 5
Experimental terminal concentration data^a

Run	$C_{d,in}$ (g/l)	$C_{d,out}$ (g/l)	$C_{c,in}$ (g/l)	$C_{c,out}$ (g/l)	Loss of solute in mass balance (%)	N_{odp}
A: Butanol–succinic acid–water						
L8	13.78	42.26 (4.4)	45.48	17.00 (1.2)	7.5	6.89
L9	11.84	46.78 (7.5)	51.64	16.70 (3.4)	11.7	6.45
L10	7.12	48.19 (8.5)	54.57	13.50 (4.2)	12.0	6.12
L11	11.68	42.40 (1.6)	47.02	16.30 (3.1)	3.8	5.64
L12	0.25	46.49 (7.7)	51.74	5.50 (3.7)	8.3	8.45
L13	7.78	47.88 (5.1)	52.80	12.70 (1.6)	6.7	7.58
B: Cumene–isobutyric acid–water						
H9	13.74	50.82 (1.2)	37.84	25.48	1.5	0.74
H10	21.89	55.86 (3.9)	37.64	26.30	6.8	0.80
H11	25.06	62.62 (0.7)	39.67	27.15	0.7	0.85
H12	24.18	66.81 (1.0)	38.23	24.00	1.1	1.23
H13	28.66	64.90 (2.8)	36.02	23.94	4.9	1.35
H14	22.63	85.60 (0.1)	45.09	24.10	0.2	1.42
H15	22.51	86.83 (0.1)	45.16	23.72	0.2	1.50
H16	18.20	68.57 (3.7)	38.09	21.30	3.1	1.68

^aValues in paranthesis denote % change proposed for perfect mass balance.

3. As Fig. 4 shows, most of the drop breakage events happen in the first few stages where larger drops exist. Static volume fraction distributions of drops are shown in Fig. 5 for a typical run.

10. Effect of drop breakage on mass transfer simulation

A problem which comes from the drop breakage process is to keep the history of different drops with respect to their contamination factor values and the inlet concentrations for each drop size class in each stage. The concentration of solute in each drop is affected by its earlier history and each drop keeps its own identity. A distinction was considered

between the drops newly formed and drops which were not broken at the previous rotor (or rotors). It was assumed that the daughter drops formed have a uniform concentration which is the same as the concentration in the mother drop just before breakage. For each sort of drops coming to class i at stage n the appropriate level of contamination was calculated by adding the term $a_1 t_{r,i,n} d_i^{a_2}$ to its previous contamination factor value according to Eq. (20). The inlet concentrations to each stage, with the appropriate residence times for each sort of drops were used in Eq. (10) for the solute transfer calculations and obtaining the concentration when leaving the stage.

Drop breakage causes a branching distribution in mass transfer simulation in which drops with similar identities go

Table 6
Calculated results of column overall Sauter mean drop size and average hold-up for mass transfer runs

Run No.	F_d (cm ³ /s)	N_r (s ⁻¹)	Experimental		Calculated	
			d_{32} (mm)	Hold-up	d_{32} (mm)	Hold-up
A: Cumene–isobutyric acid–water						
H9	13.90	4.16	2.09	0.031	2.07	0.027
H10	20.80	4.16	1.80	0.059	1.82	0.060
H11	27.75	4.16	1.94	0.090	2.09	0.094
H12	16.64	5.00	1.55	0.045	1.60	0.048
H13	20.80	5.00	1.70	0.061	1.57	0.073
H14	6.65	5.41	1.16	0.025	1.18	0.021
H15	9.97	5.41	1.23	0.036	1.15	0.038
H16	13.33	5.41	1.30	0.073	1.11	0.072
B: Butanol–succinic acid–water						
L8	59.12	0.42	1.03	0.281	1.03	0.241
L9	50.78	0.42	1.01	0.159	1.01	0.158
L10	33.73	0.42	1.06	0.082	1.06	0.075
L11	59.12	0.00	1.18	0.181	1.18	0.176
L12	42.25	0.83	0.95	0.177	0.90	0.170
L13	25.40	0.83	0.97	0.075	0.92	0.069

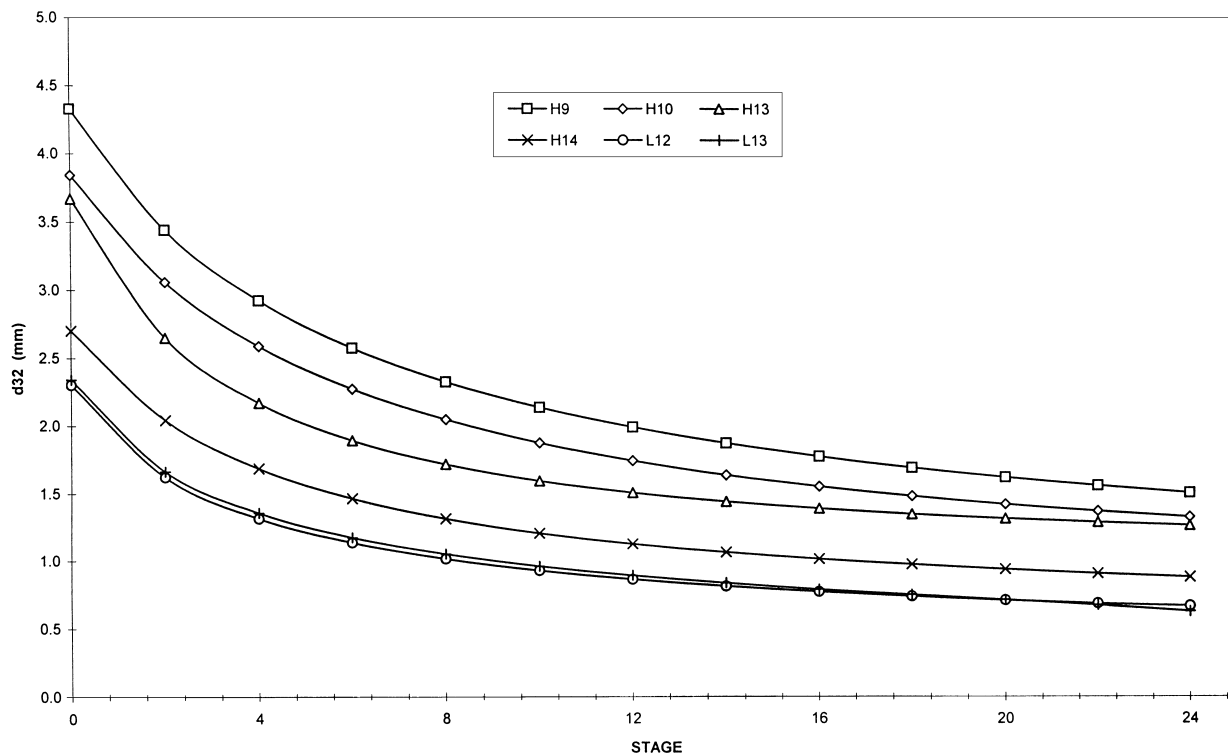


Fig. 2. Variation of Sauter mean drop size with stages for typical mass transfer runs.

to the appropriate branch. In calculations these branches were considered separately due to their different concentrations and levels of contamination. When there was no longer

significant change in hold-up or Sauter mean drop size in progressing through the stages, the few breakage events which could happen in the following stages were ignored

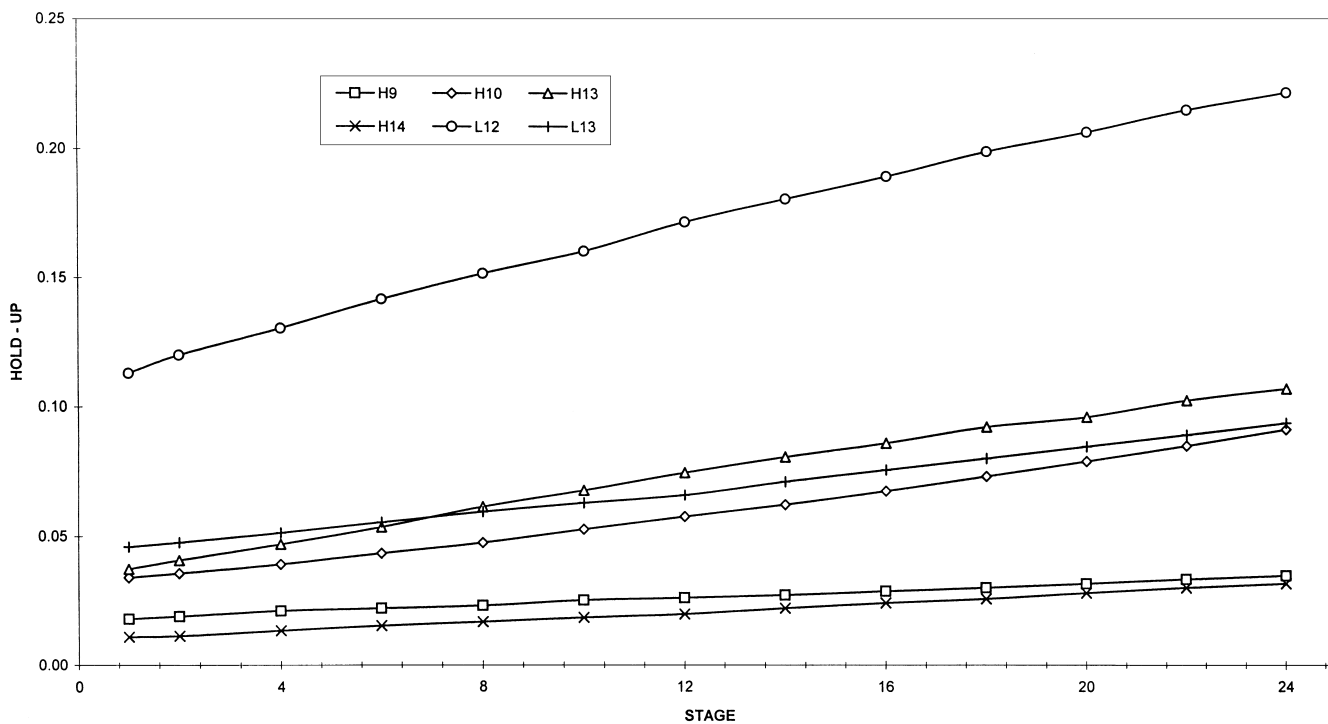


Fig. 3. Variation of hold-up with stages for typical mass transfer runs.

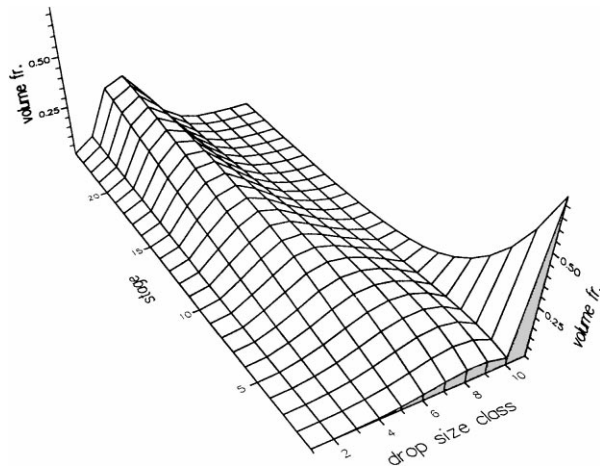


Fig. 4. Volume fraction distribution along the column for run H9.

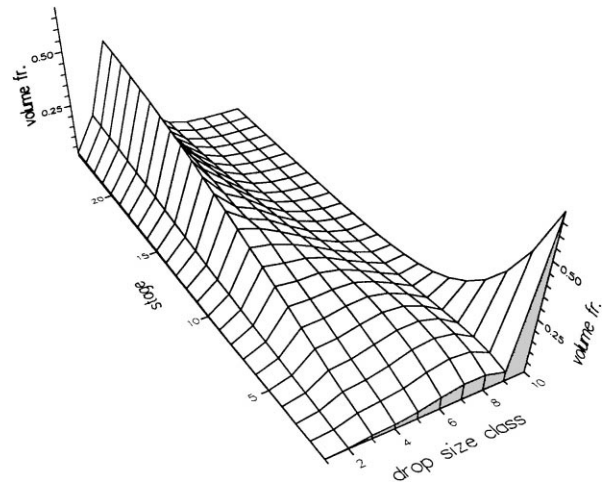


Fig. 5. Volume fraction distribution along the column for run H15.

and calculations were continued with the last obtained branches of drops to the end of the column.

11. Mass transfer simulation

The concentration profiles of the six butanol runs were best-fitted simultaneously by varying only the contamination factor equation coefficients in Eq. (20) to find one best equation. The same was done for the eight cumene runs. The way the film mass transfer coefficients vary with drop size and the increasing contamination factor along the column is shown for one run H14 in Figs. 6 and 7. The wide range of all the coefficients involved is clearly seen and the limitation of using only one average mass transfer coefficient is obvious.

Comparison of the backflow ratio values, listed in Tables 1 and 2, show that the values obtained from the Kumar-Hartland model are about 2.4 times greater

than those obtained from Misesk’s model (ignoring run L11). The best-fit coefficients for Eq. (20) in Tables 7 and 8 show that the contamination factor generated to fit the combined mass transfer model to the experimental data depends significantly on the level of axial mixing calculated using coefficients obtained from these models.

Table 7 indicates that for the butanol system and both mass transfer coefficient calculation methods and models of axial mixing, the exponent a_2 in Eq. (20) is near 1.5. Values of a_1 are about 0.06 to 0.14 according to the axial mixing correlation used. The range of m is about $0 < m < 20$, indicating moderately clean conditions at the drop interface. Slater and Hughes [39] determined contamination factor data for single drop experiments with the butanol–succinic acid–water system. For 47 data points the best fit obtained was:

$$m = 2.31td^{1.33} \quad (0 < m < 140) \quad (26a)$$

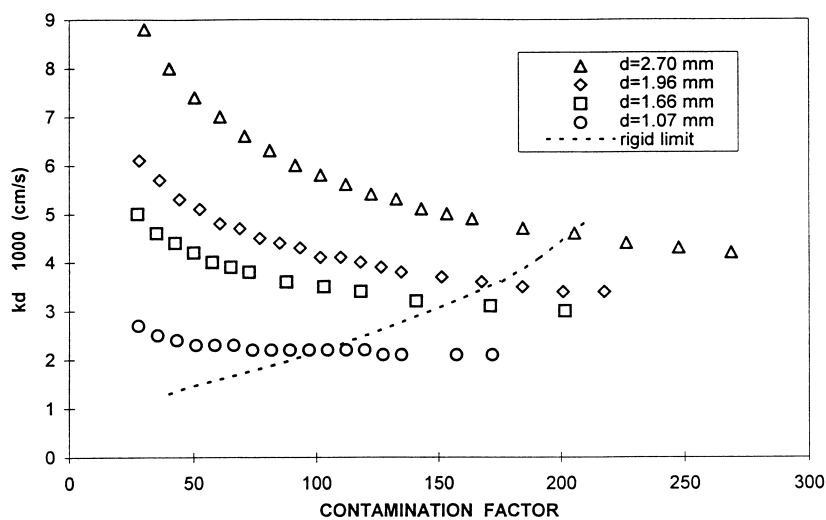


Fig. 6. Variation of k_d with contamination factor for run H14, Whitman two film theory, Kumar and Hartland model.

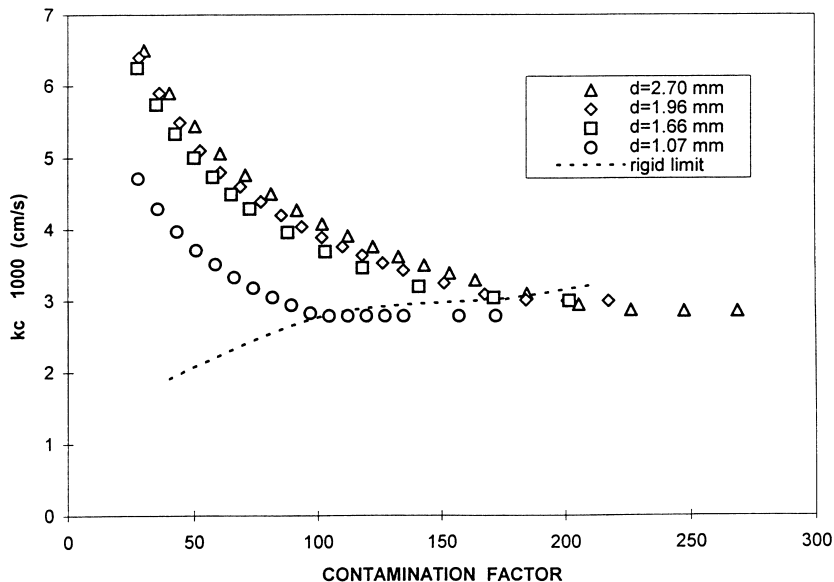


Fig. 7. Variation of k_c with contamination factor for run H14, Whitman two film theory, Kumar and Hartland model.

for drops in vertical motion, to be compared to

$$m = 0.06td^{1.5} \quad (0 < m < 20) \quad (26b)$$

for drops in the RDC, (t in s; d in mm), and for similar values of t and d .

The difference of contamination factor levels between this work and that of Slater and Hughes may be due to the following:

1. Different sources of chemicals have been used and the experiments have been carried out probably with different levels and types of contamination; however, the single drop experiments were carried out using chemicals and liquids of higher purity than used in the RDC, which should give lower values of m for single drops.
2. The concentration gradient of contaminants on drop surfaces and hence values of m may be much reduced in the RDC by virtue of drops not moving in sustained unhindered vertical motion as in experiments for which Eq. (26a) was obtained.
3. The model does not account for enhancement of mass transfer coefficients caused by agitation so values of m for the RDC are slightly lower than they should be to compensate agitation effects. This point is discussed further below.

4. Unaccounted coalescence or break-up within a compartment could give shorter drop life-times than assumed, with consequently higher mass transfer coefficients, hence smaller values of m needed to simulate results. However, neither of these processes was observed in experimental work.

The enhancement of mass transfer coefficients by agitation in RDCs has already been studied for dispersed phase film mass transfer coefficients [50] and work on continuous phase coefficients has been done (as yet unpublished). It has been found that enhancement up to 100% seems possible for drops at near critical condition, ready to break; most drops however, are much smaller than critical size at the rotor speed used so enhancement is much less. We do not understand what the enhancement might be for drops above critical size waiting to break. The effect does not seem large enough to explain the difference between Equations (26a) and (26b).

Table 8 shows the optimized values for the cumene system of coefficient $a_1 = 0.85$ and exponent $a_2 = 1.9$ (Eq. (20)) for the preferred Misesk values of the axial mixing coefficient. In this case $m_0 = 20$ is found. The range of m is about 100 to 600 indicating substantial contamination effects with drops in a near rigid condition.

Table 7
Optimised values of parameters in the contamination factor model for butanol–succinic acid–water system ($m = m_0 + a_1td^{a_2}$)^a

Axial mixing model	Kumar and Hartland		Misesk	
	a_1	a_2	a_1	a_2
Direct calculation of K_{od}	0.06	1.5	0.14	1.6
Whitman two film for K_{od}	0.02	1.6	0.08	1.7

^a $m_0 = 0$.

Table 8
Optimised values of parameters in the contamination factor model for cumene–isobutyric acid–water system ($m = m_0 + a_1td^{a_2}$)^a

Axial mixing model	Kumar and Hartland		Misesk	
	a_1	a_2	a_1	a_2
Direct calculation	1.67	1.4	0.85	1.9
Whitman two film	1.49	1.3	0.78	1.8

^a $m_0 = 20$.

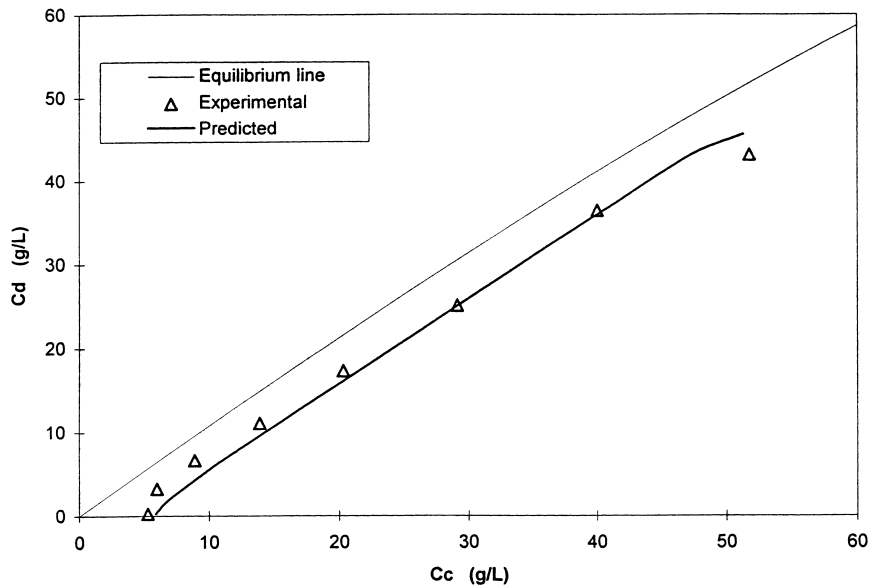


Fig. 8. Experimental and predicted operating lines for run L12, direct calculation method, Kumar and Hartland model.

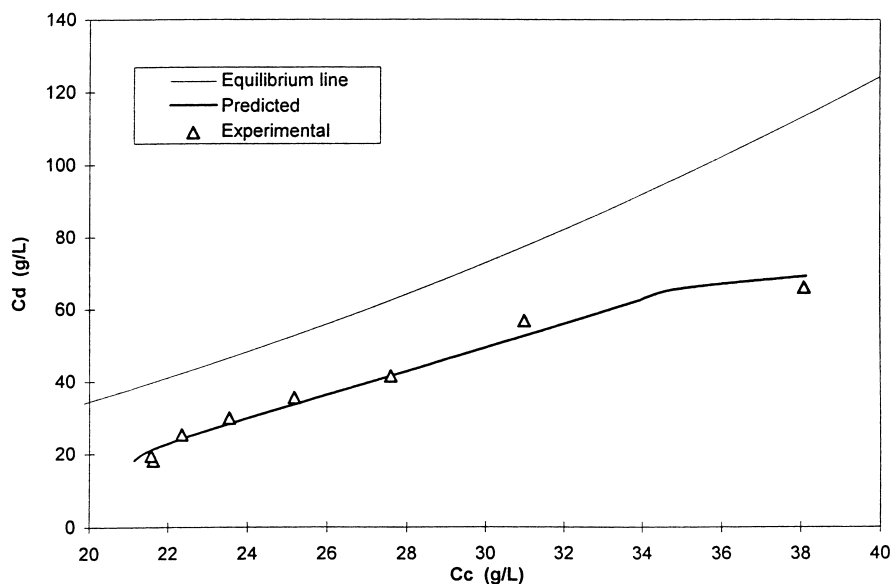


Fig. 9. Experimental and predicted operating lines for run H16, direct calculation method, Misek model.

The m values generated with the butanol–succinic acid–water system are therefore much lower than the values for the cumene–isobutyric acid–water system. The most likely reason for this difference can be attributed to the purity of chemical sources. The chemicals used in the butanol runs may be considered as clean, but for the cumene system as highly contaminated (industrial grade cumene and isobutyric acid were used). However, a matter of particular concern is that this variation of m may cover deficiencies in the combined mass transfer model in fitting experimental data. This may not be so important when designing a column using data obtained by simulating a pilot column using the same chemical system.

Finally, Figs. 8 and 9 show that the simulation of internal concentration profiles on which the conclusions reached have been based appear satisfactory.

12. Conclusions

It was found possible to fit average drop sizes and hold-up of dispersed phase for two chemical systems without using adjustable parameters for each run. The hydrodynamic equations used are well-validated for the RDC of 152 mm diameter.

A model of mass transfer coefficients which allows for effects of contamination was employed to evaluate the

significance of contamination in each of two chemical systems. The butanol–succinic acid–water system behaved as if clean but the cumene–isobutyric acid–water system behaved as if highly contaminated.

Based on single drop experimental evidence that shows that the contamination factor obtained with the combined film mass transfer model varies with time and drop size, empirical correlations for the contamination factor were determined. It is suggested that single drop experiments done to determine the contamination factor m should be carried out in a short RDC, not in an empty column because the non-uniform motion of drops in an RDC could give reduced contamination concentration gradients on drop surfaces. Enhancement of mass transfer coefficients by agitation might reasonably be attributed in part to this effect.

Drop life-times in drop swarms in the RDC need more study to gain more insight into the mass transfer process.

Two correlations for continuous phase axial mixing in the RDC were employed and it was found that the values of contamination factor obtained from concentration profiles were dependent on the axial mixing correlation used. It is important therefore to characterize axial mixing accurately if design is to be improved.

The application of a new combined model for mass transfer coefficients does not explain all aspects of the mass transfer process in an RDC. Further studies are needed to answer the questions raised.

13. Nomenclature

b	Coefficient
a_1, a_2	Contamination factor model parameters (Eq. (20))
C	Concentration (kg/m^3)
d	Drop diameter (m)
d_{CR}	Critical drop diameter for breakage (m)
d_{M}	Mother drop diameter (m)
d_{max}	Maximum stable drop diameter (m)
d_{32}	Sauter mean drop size (m)
D_{B}	Bulk diffusivity of impurity (m^2/s)
D_{c}	Molecular diffusivity in continuous phase (m^2/s)
D_{d}	Molecular diffusivity in dispersed phase (m^2/s)
D_{e}	Eddy diffusivity (m^2/s)
D_{oe}	Overall effective diffusivity (m^2/s)
D_{s}	Surface diffusivity of impurity (m^2/s)
D_{col}	Column diameter (m)
D_{r}	Rotor diameter (m)
D_{s}	Stator diameter (m)
e	Backflow ratio
E	Drop approach to equilibrium
E_{c}	Continuous phase axial mixing coefficient (m^2/s)
F	Flowrate (cm^3/s)
fr	Fraction of daughter drops
g	Acceleration due to gravity (m/s^2)
g_i	Dynamic volume fraction of drops with size d_i

h	Height of an element of column (m)
h_{c}	Compartment height (m)
H	Column height (m)
$k_{\text{ci},n}$	Continuous phase film mass transfer coefficient for drops with size d_i in stage n (m/s)
k_{d}	Drop film mass transfer coefficient (m/s)
$K_{\text{od},i,n}$	Overall dispersed phase based mass transfer coefficient for drops with size d_i in stage n (m/s)
L	A Sherwood number $k_{\text{c}}d/2\Phi D$
m	Contamination factor
m_{o}	Initial contamination factor
n	Exponent or stage number
N_{r}	Rotor speed (s^{-1})
N_{CR}	Critical rotor speed for drop breakage (s^{-1})
N_{odp}	Dispersed phase based plug-flow number of transfer units
N_{st}	Number of stages
p	Probability of breakage
r_{o}	Drop radius (m)
Re	Drop Reynolds number
Re_{k}	Drop Reynolds number using V_{k}
Sc	Schmidt number
Sh	Sherwood number
Sh_{r}	Rigid drop Sherwood number
$t_{\text{r},i}$	Residence time of drops with size d_i in a stage (s)
$V_{\text{c}}, V_{\text{d}}$	Continuous and dispersed phase superficial velocities (m/s)
\bar{V}_{c}	Continuous phase velocity relative to the column (m/s)
$V_{\text{d},i}$	Drop velocity relative to the column (m/s)
V_{k}	Drop characteristic velocity (m/s)
V_{Slip}	Slip velocity (m/s)
V_{t}	Drop terminal velocity (m/s)
V_{int}	Interfacial velocity (m/s)
We_{d}	Weber number for drop
We_{dCR}	Critical Weber number for drop
x	Dispersed phase hold-up
x_{m}	Mean number of daughter drops
y	Dimensionless drop volume

Greek symbols

α	Drop surface interfacial velocity ratio
β	Eq. (15) (kg^2/m^4)
β_{n}	Eigenvalues
δ	Film thickness (m)
ε	Kinetic coefficient for adsorption of contaminant (s^{-1})
Φ	Equilibrium curve slope ($dC_{\text{d}}/dC_{\text{c}}$)
γ	Interfacial tension (N/m)
Γ	Surface concentration of contaminant (Γ_{o} at equator) (kg/m^2)
$\mu_{\text{c}}, \mu_{\text{d}}$	Continuous and dispersed phase viscosities ($\text{kg}/\text{m s}$)
$\rho_{\text{c}}, \rho_{\text{d}}$	Continuous and dispersed phase densities (kg/m^3)

Subscripts

<i>c, d</i>	Continuous and dispersed phases
<i>i</i>	Drop size class
<i>n</i>	Stage number
<i>av</i>	Average value

Superscript

*	Equilibrium value
---	-------------------

Acknowledgements

We wish to acknowledge the support given by Dr. J.A. Grant, Department of Mathematics, University of Bradford in advancing the work done by J. Talib. We acknowledge the support of SPS, AEA Technology, in funding experimental work.

References

- [1] L. Steiner, in: J.C. Godfrey, M.J. Slater (Eds.), *Liquid-Liquid Extraction Equipment*, ch. 6, Wiley, Chichester, 1994.
- [2] G.S. Laddha, T.E. Degaleesan, *Transport Phenomena in Liquid Extraction*, McGraw-Hill, New York, 1976, pp. 1–9.
- [3] P.J. Bailes, J. Gledhill, J.C. Godfrey, M.J. Slater, Hydrodynamic behaviour of packed, rotating disc and Kühni liquid-liquid extraction columns, *Chem. Eng. Res. Des.* 64 (1986) 43–55.
- [4] A. Zimmermann, X. Joulia, C. Gourdon, A. Gorak, Maxwell-Stefan approach in extraction design, *The Chem. Eng. J.* 57 (1995) 229–236.
- [5] L. Steiner, Drop population balance: tool or flop?, *Chem. Ing. Tech.* 68(1/2) (1996) 141–146.
- [6] V. Rod, Calculating mass transfer with longitudinal mixing, *British Chem. Eng.* 11 (1966) 483–487.
- [7] T. Misek, V. Rod, in: C. Hanson (Ed.), *Recent Advances in Liquid-Liquid Extraction*, ch. 7, Pergamon Press, Oxford, 1971.
- [8] T. Misek, J. Marek, Asymmetric rotating disc contactor, *British Chem. Eng.* 15 (1970) 202–207.
- [9] H.R.C. Pratt, G.W. Stevens, in: J.D. Thornton (Ed.), *Science and Practice of Liquid-Liquid Extraction*, ch. 7, vol. 1, Clarendon Press, Oxford, 1992.
- [10] W.J. Korchinsky, S. Azimzadeh-Khatayloo, An improved stage-wise model of counter-current flow liquid-liquid extractors, *Chem. Eng. Sci.* 31 (1976) 871–875.
- [11] R.H. Chartres, W.J. Korchinsky, Modelling of liquid-liquid extraction columns: predicting the influence of drop size distribution, *Trans. Instn. Chem. Engrs.* 53 (1975) 247–254.
- [12] J.J.C. Cruz-Pinto, W.J. Korchinsky, Experimental confirmation of the influence of drop size distribution on liquid-liquid extraction column performance, *Chem. Eng. Sci.* 35 (1980) 2213–2219.
- [13] W.J. Korchinsky, R. Al-Husseini, Liquid-liquid extraction column (RDC) model parameters from drop size distribution and solute concentration measurements, *J. Chem. Techn. Biotechnol.* 36 (1986) 395–409.
- [14] W.J. Korchinsky, A.M. Ismail, Mass transfer parameters in rotating disc contactors: influence of column diameter, *J. Chem. Techn. Biotechnol.* 43 (1988) 147–158.
- [15] W.J. Korchinsky, D. Bastani, Application of forward mixing model to the low interfacial tension system *n*-butanol-succinic acid-water in rotating disc contactor liquid extraction columns, *J. Chem. Techn. Biotechnol.* 58 (1993) 113–122.
- [16] S.H. Zhang, S.C. Yu, Y.C. Zhou, Y.F. Su, A model for liquid-liquid extraction column performance: the influence of drop size distribution on extraction efficiency, *Can. J. Chem. Eng.* 63 (1985) 212–226.
- [17] J.A. Hamilton, H.R.C. Pratt, Droplet coalescence and breakage rates in a packed liquid extraction column, *A. I. Ch. E. J.* 30 (1984) 442–450.
- [18] M.O. Garg, H.R.C. Pratt, Measurement and modelling of droplet coalescence and breakage in a pulsed plate extraction column, *A. I. Ch. E. J.* 30 (1984) 432–441.
- [19] Q. Yu, J. Wang, Modelling of mass transfer in extraction columns with drop forward mixing and coalescence-redispersion, *Can. J. Chem. Eng.* 70 (1992) 88–96.
- [20] C. Gourdon, G. Casamatta, G. Muratet, in: J.C. Godfrey, M.J. Slater (Eds.), *Liquid-Liquid Extraction Equipment*, ch. 7, Wiley, Chichester, 1994.
- [21] K. Arimont, M. Soika, M. Henschke, Simulation of a pulsed packed extraction column, *Chem. Ing. Tech.* 68(3) (1996) 276–279.
- [22] B. Hoting, A. Vogelpohl, Fluid dynamics and mass transfer in extraction columns with structured packings, *Chem. Ing. Tech.* 68(1/2) (1996) 105–109 and 109–113.
- [23] J. Talib, Ph.D Thesis, University of Bradford, 1994.
- [24] J.S. Ghalehchian, PhD thesis, University of Bradford, 1996.
- [25] D.K. Chang-Kakoti, W.-Y. Fei, J.C. Godfrey, M.J. Slater, Drop sizes and distributions in rotating disc contactors used for liquid-liquid extraction, *J.Sep. Proc. Technol.* 6 (1985) 40–48.
- [26] V. Cauwenberg, P. Van-Rompay, Z.Q. Mao, M.J. Slater, The breakage of drops in rotating disc contactors, in: *Proc. ISEC 93*, vol. 1, Elsevier, Amsterdam, 1993, pp. 421–428.
- [27] J.C. Godfrey, M.J. Slater, Slip velocity relationships for liquid-liquid extraction columns, *Trans. I. Chem. E.* 69 (1991) 130–141.
- [28] N.L. Ricker, F. Nakashio, C.J. King, An efficient general method for computation of counter-current separation processes with axial dispersion, *A. I. Ch. E. J.* 27 (1981) 277–284.
- [29] W.J. Korchinsky, in: J.C. Godfrey, M.J. Slater (Eds.), *Liquid-Liquid Extraction Equipment*, ch. 9, Wiley, Chichester, 1994.
- [30] M.J. Slater, in: J.C. Godfrey, M.J. Slater (Eds.), *Liquid-Liquid Extraction Equipment*, ch. 4, Wiley, Chichester, 1994.
- [31] M.J. Slater, A combined model of mass transfer coefficients for contaminated drop liquid-liquid systems, *Can. J. Chem. Eng.* 73 (1995) 462–469.
- [32] A.C. Lochiel, The influence of surfactants on mass transfer around spheres, *Can. J. Chem. Eng.* 43 (1965) 40–44.
- [33] L. Steiner, Mass transfer rates for single drops and drop swarms, *Chem. Eng. Sci.* 41 (1986) 1979–1986.
- [34] G.E. Kinard, F.S. Manning, W.P. Manning, A new correlation for mass transfer from single spheres, *British Chem. Eng.* 8 (1963) 326–327.
- [35] A.E. Handlos, T. Baron, Heat and mass transfer from drops in liquid-liquid extractors, *A. I. Ch. E. J.* 3 (1957) 127–136.
- [36] M. Hubis, S. Hartland, Limitations of the Handlos-Baron model, *Chem. Eng. Sci.* 41 (1986) 2436.
- [37] C.H. Young, W.J. Korchinsky, Modelling drop side mass transfer in agitated polydispersed liquid-liquid systems, *Chem. Eng. Sci.* 44 (1989) 2355–2361.
- [38] J. Temos, H.R.C. Pratt, G.W. Stevens, Comparison of tracer and bulk mass transfer coefficients for droplets, in: *Proc. ISEC 93*, Elsevier, Amsterdam, 1993, pp. 1770–1777.
- [39] M.J. Slater, K.C. Hughes, The application of a new combined film mass transfer coefficient model to the *n*-butanol/succinic acid/water system, in: *Proc. ISEC 93*, Elsevier, Amsterdam, 1993, pp. 1238–1245.
- [40] V. Alessi, C. Gradella, R. Penzo, M.J. Slater, The application of a new combined mass transfer coefficient model to an industrial extraction system subject to contamination, in: *Proc. ISEC 93*, Elsevier, Amsterdam, 1993, pp. 1095–1102.

- [41] T. Miyauchi, T. Vermeulen, Diffusion and backflow models for two-phase axial dispersion, *Ind. Eng. Chem. Fund.* 2 (1963) 304–310.
- [42] T. Misek, Backmixing in full-scale ARD and RDC extractors, *Coll. Czech. Chem. Commun.* 40 (1975) 1686–1693.
- [43] A. Kumar, S. Hartland, Prediction of axial mixing coefficients in RDC and ARDCs, *Can. J. Chem. Eng.* 70 (1992) 70–87.
- [44] P.J. Bailes, J.C. Godfrey, M.J. Slater, Liquid–liquid extraction test systems, *Chem. Eng. Res. Des.* 61 (1983) 321–324.
- [45] H. Bahmanyar, D.R. Dean, I.C. Dowling, K.M. Ramlochan, M.J. Slater, W. Yu, Studies of drop break-up in liquid–liquid systems in an RDC, *Chem. Eng. Technol.* 14 (1991) 178–185.
- [46] H. Bahmanyar, M.J. Slater, Studies of drop break-up in liquid–liquid systems in an RDC, *Chem. Eng. Technol.* 14 (1991) 79–89.
- [47] V. Cauwenberg, Ph.D. Thesis, Katholieke University Leuven, Belgium, 1995.
- [48] V. Cauwenberg, J. Degreve, M.J. Slater, The interaction of solute transfer, contaminants and drop break-up in rotating disc contactors: Part 1. Correlation of drop breakage probabilities and Part 2. The coupling of the mass transfer and breakage processes via interfacial tension, *Can. J. Chem. Eng.* 75 (1997) 1046–1055 and 1056–1066.
- [49] R.A. Mugele, H.D. Evans, Droplet size distribution in sprays, *Ind. Eng. Chem.* 43 (1951) 1317–1324.
- [50] H. Bahmanyar, D.K. Chang-Kakoti, L. Garro, T.-B. Liang, M.J. Slater, Mass transfer from single drops in rotating disc, pulsed sieve plate and packed liquid–liquid extraction columns, *Trans. IChemE*, 68A (1990) 74–83.